Replies to both reviewer comments are below, followed by a marked-up version of the manuscript.

Author comment 1.

We thank both reviewers for their constructive and helpful comments on this article.

Interactive comment on "Chemistry-climate model simulations of the Mt. Pinatubo eruption using

CCMI and CMIP6 stratospheric aerosol data" by Laura Revell et al.

M. Toohey (Referee)

This manuscript describes coupled chemistry climate model simulations utilizing two different volcanic forcing data sets, and explores differences in the simulated responses to the volcanic forcing, including stratospheric temperatures, circulation and ozone. The experimental set-up is clear, and the results show that the stratospheric temperature anomalies produced by the newer CMIP6 volcanic forcing reconstruction are in closer agreement to observations. The paper also provides information regarding the construction of the CMIP6 forcing data, which is presently not available elsewhere. I find the work to be well within the scope of ACP, and the conclusions to be in general well justified by the results shown. I have a few minor comments I encourage the authors to consider before publication.

General comments

1. The results of the study focus almost exclusively on the tropics. Extratropical ozone changes in the SH are mentioned in passing, but there is no analysis of extratropical NH ozone changes (which seem to be positive for both forcing sets, inconsistent with observations), or polar temperatures (despite large changes in the forcing at high latitudes), etc. However, the title is very general, and some statements throughout the manuscript could be construed as applying to the stratosphere as a whole, rather than just the tropics (see specific comments below). I suggest the title be changed to reflect the concentration on the tropics, and some care be taken to be clear about the specificity of the results.

We have changed the title to: "Impacts of Mt. Pinatubo volcanic aerosol on the tropical stratosphere in chemistry-climate model simulations using CCMI and CMIP6 stratospheric aerosol data."

2. The introduction mentions the wide range simulated temperature and ozone responses to volcanic forcing in the CCMVal activity. But since the CMIP6 volcanic forcing data set is nominally an update to forcings used in past CMIP activities, it would make sense to briefly review the simulated responses to volcanic forcing in past CMIPs. Charlton-Perez et al. (2013) show CMIP5 global mean stratospheric temperature changes associated with Pinatubo split into high-and low-top models, and Driscoll et al. (2012) show tropical temperature anomalies, split into groups of models using different forcing reconstructions. Toohey et al. (2014) compare temperature and circulation anomalies from the Stenchikov forcing (basically equivalent to the Sato et al. (1993) forcing used in many CMIP5 models) and the CCMI (SAGE-4) forcing.

Thank you for bringing these papers to our attention; we thought that Driscoll et al. (2012) was most relevant for the study at hand and we have included the range of CMIP5 tropical temperature anomalies in the introduction:

"However, model simulations of the Mt. Pinatubo eruption are diverse. For example, GCMs participating in phase 5 of the Coupled Model Intercomparison Project (CMIP5) simulated tropical (30 °N–30 °S) temperature anomalies at 50 hPa ranging between 2–10 K (Driscoll et al., 2012). Similarly, CCMs participating in CCMVal-2, the predecessor activity to phase 1 of the Chemistry-Climate Model Initiative (CCMI-1), simulated global-mean temperature anomalies between -1 K and +9 K at 50 hPa in the post-Pinatubo eruption period, and global-mean ozone anomalies between -2% and -22% (Mancini et al., 2010)."

3. In a few places, the authors draw a direct line of causation from heating of the tropical lower stratosphere and increased tropical upwelling, and in some cases, link this further with increases in extratropical downwelling. While this may be true, there is also evidence of post-volcanic changes in extratropical large-scale wave breaking in observations (Graf et al., 2007; Poberaj et al., 2011) and model results (Bittner et al., 2016; Toohey et al., 2014). This increased wave breaking should increase transport from the tropics to extratropics, and induce residual circulation anomalies. I think there is still a low degree of understanding on how the related processes of enhanced wave-breaking and tropical heating affect stratospheric tropical upwelling, extratropical mixing and downwelling. The issue of causation is not central to this study, so I'm not necessarily suggesting a detailed review of the topic, but I encourage the authors to not oversell the understanding of the mechanistic explanation of circulation changes, for example in the Introduction (p2, l24), results (p7, ll10-13) and Conclusions (p8, l29).

We have taken care to moderate our discussion on the links between heating and upwelling, e.g.:

"Heating in the tropical stratosphere is thought to drive an increase in the rate of tropical upwelling (Rosenfield et al. 1997), indicated by an increase in the residual vertical velocity w* (Fig. 2b), which is a useful proxy for the strength of the Brewer-Dobson circulation."

4. Pedantic semantic comment: these are not really simulations of the Mt. Pinatubo eruption (as stated in the title and throughout the document), they are rather simulations of the atmospheric response to stratospheric aerosols resulting from the Mt. Pinatubo eruption. This is of course obvious to many readers, but can be confusing to readers new to the field.

Good point and we hope that the new title, and various changes throughout the manuscript, will be less confusing to readers new to the field.

Specific comments

P1, l9: suggest "uses measurements from CLAES (: : :) on UARS, the: : :"

Changed as suggested:

"For CMIP6, the new "SAGE-3λ" data set was compiled, which excludes the least reliable SAGE II wavelength and uses measurements from CLAES (Cryogenic Limb Array Etalon Spectrometer) on UARS, the Upper Atmosphere Research Satellite, for gap-filling following the Mt. Pinatubo eruption instead of ground-based Lidars."

P1, l14: this overestimated heating and ozone loss is specifically in the lower tropical stratosphere. Comparisons of extratropical temperatures and ozone are not shown.

We have clarified that the overestimations apply only to the tropical lower stratosphere:

"The use of SAGE-4λ results in heating and ozone loss being overestimated in the tropical lower stratosphere compared to observations in the post-eruption period by approximately 3 K and 0.2 ppmv, respectively."

P1, l17: Again, this applies only to tropical temperatures.

We have clarified this in the text:

"As a result, simulated tropical temperature anomalies in the model simulations based on SAGE-3λ for CMIP6 are in excellent agreement with MERRA and ERA-Interim reanalyses in the post-eruption period."

P1, l20: This ozone loss is specific to 30 hPa, 15°S-15°N I believe, and is a peak value I guess?

Yes, we have now noted that the ozone loss is overestimated by up to 0.1 ppmv:

"Ozone loss following the Mt. Pinatubo eruption is overestimated by up to 0.1 ppmv in the model simulations based on SAGE-3λ, which is a better agreement with observations than in the simulations based on SAGE-4λ."

P2, l2: I think the IR absorption by aerosols was known about, and reasonably well understood before 2013.

True, although the IPCC assessments provide a good summary of the current state of knowledge for readers new to the field. We have amended this to "see e.g. Boucher et al. (2013) and references therein."

P2, l15: The last sentence here is a strong statement, which could use some support from prior work. Son et al. (2010) comes to mind, but there are surely other references that would support this.

We have cited Son et al. (2010) here.

P2, l26: This statement is supported by two pretty random references from a great sea of literature. At the very least, an "e.g." is called for, otherwise review articles (e.g., Robock, 2000; Timmreck, 2012) would seem to be a better fit.

Changed as suggested:

"Because aerosols play such an important role in Earth's climate, as observed from past volcanic eruptions e.g. (Robock, 2000; Solomon et al., 2011; Guillet et al., 2017)..."

P3, l13: I don't think the analysis of tropical lower stratospheric temperatures really constitutes an investigation of "climate".

Changed to "stratospheric chemistry and temperatures."

P4, l13-20: Some more details regarding the correction are needed. It is written that the issue pertains to the "extra-tropical lowermost stratosphere", but later the correction is applied "below 20 km", is this at all latitudes or only in the extratropics? It is written the correction applies to H2SO4 mass, should this not affect IR absorption then, which is roughly proportional to aerosol mass?

The correction is an altitude-dependent value (shown in Figure 1 below), applied everywhere irrespective of season or latitude, and increases SAD by the amount shown in Figure 1. These small particles (i.e. the SAD included by the correction) are included in the model's chemistry scheme but are not considered in the radiative calculations. We took only the contribution of the log-normal distribution for both longwave and shortwave. The comparison of extinctions at 3.46 μm shows good agreement with HALOE data in the stratosphere.

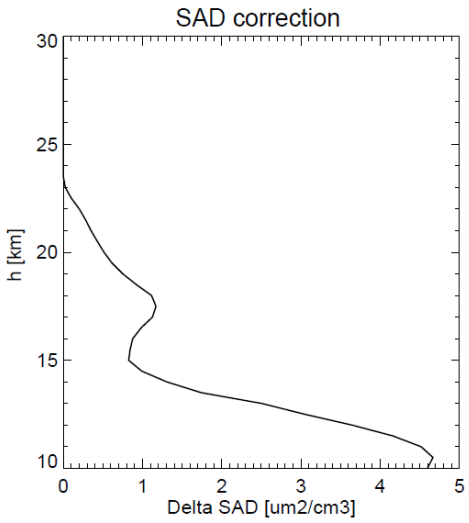

Figure 1: the SAD OPC correction applied to SAGE-3λ data.

P4, l31-: This got confusing for me. If n, r and σ are found in step 1, what are the "remaining two parameters" mentioned in step 2? And with some constructed relationships between k_{1020} and r_{eff} and σ, how can you use these to calculate number density (p5, l2)? I really wonder how one can retrieve 3 pieces of information (n, r and σ) from measurements at a single wavelength, there must be some assumptions that go into this reconstruction.

In step 1 we obtained three parameters (n, r and σ) using only three input values (extinction coefficients at three wavelengths for CMIP6 aerosols/4 wavelengths for CCMI aerosols), which are partially correlated. A small measurement error of input values may cause large excursions of the output parameters (n, r, σ). Therefore, we use a σ -k_{1020} correlation in CMIP6 to minimize the effects introduced by the measurement errors, even during the SAGE II time, where extinction coefficients at 3 wavelengths were available. This correlation is obtained from the output of step 1.

For some time periods, extinction coefficients at only one wavelength were available (from satellite instruments or photometers). Both correlations (σ - k_{1020} and r_{eff}–k_{1020}), again obtained from the SAGE II time period, were used to calculate the remaining unknown parameter, the number density.

We have rewritten Section 2.3 as:

"The SAGE-4λ and SAGE-3λ algorithms were used in the CCMI and CMIP6 data sets, respectively. In both cases, a lognormal size distribution of stratospheric aerosol is assumed. For a single mode lognormal distribution, three parameters (number density n, mode radius r and width σ) are required. Both the SAGE-3λ and SAGE-4λ algorithms consist of two steps for calculating n, r and σ:

1) Obtain n, r and σ by fitting the SAGE II extinction coefficients at four wavelengths (385, 452, 525 and 1024 nm) for the CCMI data set and three wavelengths for the CMIP6 data set. The data

uncertainty at 385 nm is much higher than for the other three wavelengths, for two reasons. Firstly, the molecular extinction at shorter wavelengths is higher than at longer wavelengths. Therefore the removal of the signal of air molecules is much more difficult. Secondly, the extinction at 385 nm is also affected by gas phase absorption. Therefore, in the more recent CMIP6 data set, the extinction coefficients at 385 nm are excluded.

2) In step 1, n, r and σ were obtained using the extinction coefficients at three wavelengths for the CMIP6 data set, and four wavelengths for the CCMI data set, which are partially correlated. However, a small measurement error on the input values may cause large inaccuracies in the output parameters (n, r and σ). Therefore a σ –k1020 correlation was used in the CMIP6 data set to minimize the effects introduced by the measurement errors, even during the SAGE II period, where extinction coefficients at three wavelengths were available. This correlation is obtained from the output of step 1. In CCMI, the r_{eff}–k_{1020} correlation was used to obtain r. The remaining two parameters (n and σ) were obtained by fitting to the measured extinction coefficients. The fitting quality remains almost as good as step 1.

For other time periods (outside the SAGE II period), extinction coefficients at only one wavelength were available (from satellite instruments or photometers). Both correlations (σ –k_{1020} and r_{eff}–k_{1020}), again obtained from the SAGE II time period, were used to calculate the remaining unknown parameter, the number density. The radiative properties (extinction coefficients, single scattering albedos and asymmetry factors) for model wavelength bands were then calculated using Mie theory (Bohren and Huffman, 2007). For SOCOLv3 this procedure was executed for 6 wavelength bands in the shortwave range (solar radiation) and 16 in the longwave range (terrestrial radiation).”

P5, l16: “: : :derive heating rates.” But also scattering, atmospheric transmission, etc.

Changed as suggested:

“Aerosol radiative effects are calculated within SOCOLv3 by using pre-calculated extinction coefficients, asymmetry factors and single scattering albedos for each spectral band to derive radiative heating rates, scattering and atmospheric transmission.”

P6, l2: The simulations are free-running, but what about the QBO? The temperature anomalies in Fig 4 seem to be oscillating quasi biennially, with the simulations right in line with the observations.

Yes, the QBO is nudged to observations. We added:

“Although the REF-C1 simulation is free-running, in SOCOLv3 the quasi-biennial oscillation (QBO) is forced by nudging the zonal tropical stratospheric winds (20° N—20° S, 3-90 hPa) to a time series of observed wind profiles (Giorgetta et al. 1996, Stenke et al. 2013).”

P6, l28-30: This last sentence seems at least misplaced (in this subsection on the aerosol mass comparison), and also not well supported by any results shown here.

We have removed this sentence.

P8, l14: Focusing on a single height level always runs the risk of sampling error. Observed temperature anomalies after Pinatubo appear to peak around 20 hPa, slightly higher than most simulations (see Fig 1 of Toohey et al., 2014). Just to be sure that 30 hPa is telling the right (and/or full) story, it would really be great to include a latitude/height cross section of zonal mean temperature anomalies (and perhaps ozone too).

Zonal-mean temperature and ozone anomalies from reanalyses/observations are shown as a function of pressure and latitude in Figure 2 below (panels a-c), and we will include these in a supplementary figure to the paper. These show that 30 hPa is an appropriate pressure level to focus on for our time series plots, with both reanalyses showing peak temperature anomalies at 20-30 hPa (a-b) and SWOOSH observations showing maximum ozone decreases at 30 hPa (c).

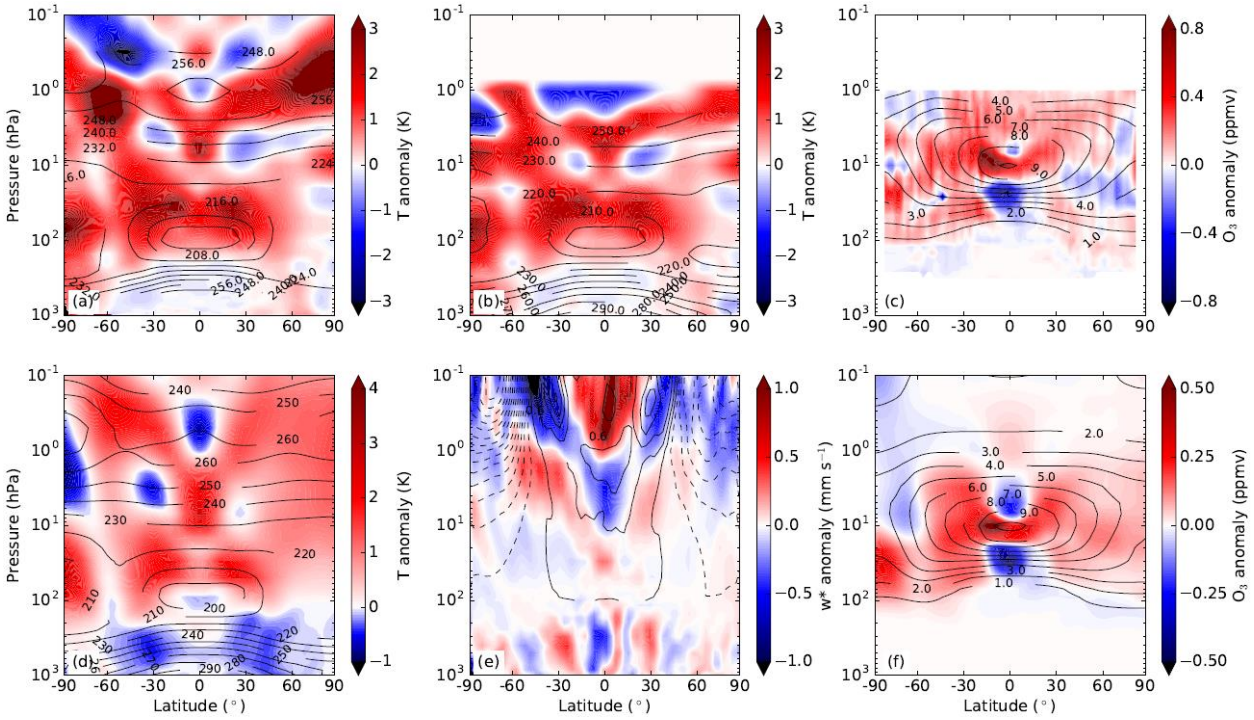

Figure 2: Top row: Anomalies in the 6 months following the Mt. Pinatubo eruption for (a) MERRA temperature reanalyses; (b) ERA-Interim temperature reanalyses; (c) SWOOSH ozone observations. Black contour lines show the annual climatological mean (1986-2005). Bottom row: Ensemble-mean, zonal-mean anomalies averaged over the 6 months following the Mt. Pinatubo eruption for the simulations using CMIP6 aerosol. (a) Temperature anomalies in the CMIP6 ensemble (red/blue shading). Black contours indicate the annual climatological mean (1986-2005) temperatures for the

CMIP6 ensemble. (b) As for (a), but showing anomalies in the rate of the vertical residual circulation (w*). For clarity, the annual climatological mean rate of the vertical residual circulation (black contours) is only shown above 100 hPa. Dashed contours indicate negative values. (c) As for (a), but showing ozone anomalies.

P8, l31: the temperature and ozone anomalies quoted here are specific to locations and times.

We have clarified that these refer to tropical stratospheric anomalies following the Mt. Pinatubo eruption:

"In the simulations using the SAGE-4λ stratospheric aerosol data set developed for CCMI, tropical stratospheric warming following the Mt. Pinatubo eruption is overestimated by approximately 3 K compared to reanalyses, and local reductions in ozone are overestimated by approximately 0.2 ppmv."

P9, l7: suggest "tropical stratospheric temperature: : :"

Changed as suggested.

Fig 1: It's hard to read anything quantitative from the color scale used in this plot. Perhaps percent difference (CMIP6-CCMI)/CCMI would work better?

This figure has been updated as suggested:

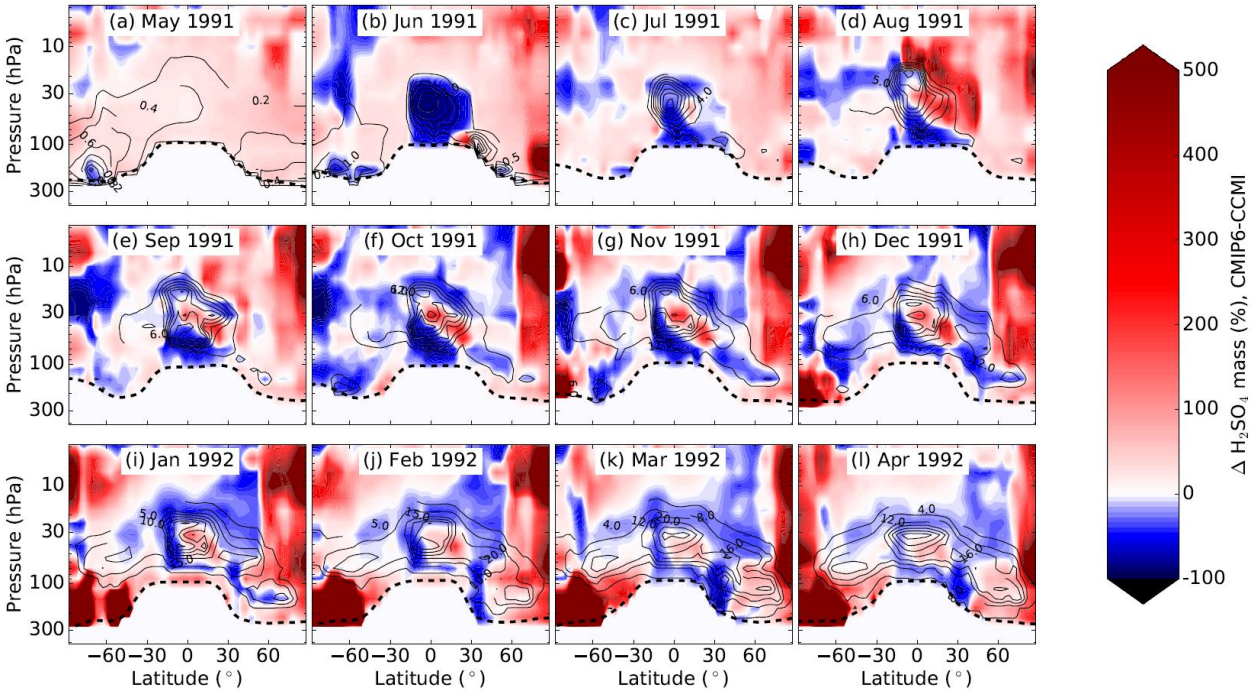

Figure 3: Percent difference in H_2SO_4 aerosol mass in the CCMI and CMIP6 stratospheric aerosol data sets for 12 months around the Mt. Pinatubo eruption in June 1991, CMIP6 minus CCMI. Black contours show the CCMI H2SO4 mass in 10^9 molecules cm^{-3}. The dashed black line shows the location of the WMO-defined tropopause. Note that aerosol data are supplied down to 5 km altitude in the CCMI and CMIP6 data sets, which are based on cloud-cleared SAGE II measurements, but these values are recommended for use only above the model tropopause.

Fig 3: Showing the results of the CMIP6 simulations as a difference plot wrt the CCMI forcing is very useful, but on the other hand, it would also be nice to see the results in their absolute values. Many potentially interesting results are hard to glean from only the difference plot, for example, it's clear that the upwelling in the lower tropical stratosphere is decreased in the CMIP6 simulations compared to CCMI, but it's not obvious then what the magnitude of the upwelling anomaly is in the CMIP6 simulation ensemble. Such a plot could (rather easily I assume) be added to the main text or included as a supplement.

We have prepared a figure showing the absolute values for the CMIP6 simulations to include in the supplement; see Figure 2 above, panels d-f.

Author comment 2.

Interactive comment on "Chemistry-climate model simulations of the Mt. Pinatubo eruption using CCMI and CMIP6 stratospheric aerosol data" by Laura Revell et al.

Anonymous Referee #2

In this manuscript the authors compare the results of SOCOLv3 simulations performed using the SAGE-4λ and SAGE-3λ stratospheric aerosol datasets, used for the CCMI-1 and CMIP-6 model intercomparisons, respectively. In particular, the authors compare the temperatures and ozone concentrations during the post-Pinatubo period in the two simulation ensembles to each other and to the MERRA and ERA-Interim reanalysis. I have found this an interesting paper, well-written and logically organized. It is a good paper that represent a necessary reference to document the differences between the two datasets. I have only some minor comments:

- page 3 line 13: "we investigate the impact of the Mt. Pinatubo eruption on climate and stratospheric chemistry". The authors only show changes in temperature and w, too little to speak about changes in climate. I would explicitly write "we investigate the impact of the Mt. Pinatubo eruption on stratospheric temperatures and chemistry".*

Changed as suggested.

- section 2.3 is not very clear. Starting from the title, I would spell out the full names of the databases: "The SAGE-3λ and SAGE-4λ". Initially I wondered if the authors where introducing a third database that merges SAGE-3λ and SAGE-4λ. Secondarily, I do not understand the steps. Step 1 is the calculation of n, r, and σ from the different wavelengths. But what is step 2? Which correction is calculated? Or did you mean "correlation"? Also, what are the remaining two parameters, n and σ? But they have already been obtained in step 1.

We have changed the title of this section as suggested. And yes, "correlation" was meant rather than "correction" – thanks for bringing this error to our attention! Step 2 describes how n and σ can be obtained from the correlation even when SAGE II data are not available. We have rewritten step 2 as:

"In step 1, *n*, *r* and σ were obtained using the extinction coefficients at three wavelengths for the CMIP6 data set, and four wavelengths for the CCMI data set, which are partially correlated. However, a small measurement error on the input values may cause large inaccuracies in the output parameters (*n*, *r* and σ). Therefore a σ -k_{1020} correlation was used in the CMIP6 data set to minimize the effects introduced by the measurement errors, even during the SAGE II period, where extinction coefficients at three wavelengths were available. This correlation is obtained from the output of step 1. In CCMI, the r_{eff}-k_{1020} correlation was used to obtain *r*. The remaining two parameters (*n* and σ) were obtained by fitting to the measured extinction coefficients. The fitting quality remains almost as good as step 1.

For other time periods (outside the SAGE II period), extinction coefficients at only one wavelength were available (from satellite instruments or photometers). Both correlations (σ -k_{1020} and r_{eff}-k_{1020}), again obtained from the SAGE II time period, were used to calculate the remaining unknown parameter, the number density."

- figure 4: The authors compare with MERRA and ERA-Interim to establish which one of the two databases lead to better simulations. However, reanalysis might not be the best tool to evaluate a model after a volcanic eruption, as they are driven by satellite data which might not be reliable after such strong perturbation. Additionally, they might not respond correctly to such a strong and sudden perturbation. I would suggest to add a comparison to measurements, many of which as cited in the introduction.

We note that the reanalyses assimilate all available data, not just satellite data. Further, Dee et al. (2011) note that in ERA-Interim they apply a bias correction which avoids some of the problems encountered in the post-Pinatubo eruption period in the ERA-40 reanalysis. Zonal-mean latitude/pressure cross-sections of temperature anomalies in the MERRA and ERA-Interim reanalyses (Figure 2a-b) shows warming in the tropical lower stratosphere of ~3 K, which, given that this is a 6-monthly average, is in good agreement with the "up to 3.5 K" warming reported by Labitzke and McCormick, 1992 (cited in the introduction).

Impacts of Mt. Pinatubo volcanic aerosol on the tropical stratosphere in chemistry-climate model simulations using CCMI and CMIP6 stratospheric aerosol data

Laura Revell[1,2], Andrea Stenke[2], Beiping Luo[2], Stefanie Kremser[3], Eugene Rozanov[2,4], Timofei Sukhodolov[4], and Thomas Peter[2]

[1]Bodeker Scientific, Christchurch, New Zealand
[2]Institute for Atmospheric and Climate Science, ETH Zurich, Zurich, Switzerland
[3]Bodeker Scientific, Alexandra, New Zealand
[4]Physical-Meteorological Observatory/World Radiation Center, Davos, Switzerland

Correspondence to: Laura Revell (laura@bodekerscientific.com)

Abstract. To simulate the impacts of volcanic eruptions on the stratosphere, chemistry-climate models that do not include an online aerosol module require temporally and spatially resolved aerosol size parameters for heterogeneous chemistry and aerosol radiative properties as a function of wavelength. For phase 1 of the Chemistry-Climate Model Initiative (CCMI-1) and, later, for phase 6 of the Coupled Model Intercomparison Project (CMIP6) two such stratospheric aerosol data sets were compiled, whose functional capability and representativeness are compared here. For CCMI-1, the "SAGE-4λ" data set was compiled, which hinges on the measurements at four wavelengths of the SAGE (Stratospheric Aerosol and Gas Experiment) II satellite instrument and uses ground-based Lidar measurements for gap-filling immediately after the Mt. Pinatubo eruption, when the stratosphere was optically opaque for SAGE II. For CMIP6, the new "SAGE-3λ" data set was compiled, which excludes the least reliable SAGE II wavelength and uses **measurements from** CLAES (Cryogenic Limb Array Etalon Spectrometer) ~~measurements~~ on UARS, the Upper Atmosphere Research Satellite, for gap-filling following the Mt. Pinatubo eruption instead of ground-based Lidars. Here, we performed SOCOLv3 (Solar Climate Ozone Links version 3) chemistry-climate model simulations of the recent past (1986–2005) to investigate the impact of the Mt. Pinatubo eruption in 1991 on stratospheric temperature and ozone and how this response differs depending on which aerosol data set is applied. The use of SAGE-4λ results in heating and ozone loss being overestimated in the **tropical** lower stratosphere compared to observations in the post-eruption period by approximately 3 K and 0.2 ppmv, respectively. However, less heating occurs in the model simulations based on SAGE-3λ, because the improved gap-filling procedures after the eruption lead to less aerosol loading in the tropical lower stratosphere. As a result, simulated **tropical** temperature anomalies in the model simulations based on SAGE-3λ for CMIP6 are in excellent agreement with MERRA and ERA-Interim reanalyses in the post-eruption period. Less heating in the simulations with SAGE-3λ means that the rate of tropical upwelling does not strengthen as much as it does in the simulations with SAGE-4λ, which limits dynamical uplift of ozone and therefore provides more time for ozone to accumulate in tropical mid-stratospheric air. Ozone loss following the Mt. Pinatubo eruption is overestimated by **up to** 0.1 ppmv in the model simulations based on SAGE-3λ, which is a better agreement with observations than in the simulations based on SAGE-4λ.

Overall, the CMIP6 stratospheric aerosol data set, SAGE-3λ, allows SOCOLv3 to more accurately simulate the post-Pinatubo eruption period.

1 Introduction

The stratospheric aerosol layer is a key component of the climate system as it directly affects how incoming solar radiation is scattered in Earth's atmosphere and therefore affects the solar energy input to the climate system. While this scattering leads to cooling at Earth's surface, a warming occurs in the lower stratosphere because the aerosol particles absorb outgoing terrestrial radiation **(see e.g. Boucher et al. (2013) and references therein)**. In addition to radiative effects, stratospheric aerosol particles also provide the surface for heterogeneous chemical reactions that alter the chemical composition of the stratosphere. Heterogeneous chemical reactions convert active, ozone-destroying nitrogen oxides (NO_x=NO+NO_2) to nitric acid (HNO_3), which is a relatively long-lived reservoir for nitrogen species, therefore gas-phase NO_x-induced ozone destruction slows. However, with anthropogenically enhanced background concentrations of stratospheric chlorine, the efficiency of the catalytic chlorine cycles increases and overcompensates the slowing of the NO_x cycle due to a reduction of chlorine deactivation into the reservoir species $ClONO_2$ (Kinnison et al., 1994; Tie and Brasseur, 1995; Pitari et al., 2014; Muthers et al., 2015). The efficiency of the catalytic chlorine cycles is further increased by chlorine activation on aerosols under very cold conditions (polar regions or close to the tropical tropopause), i.e. heterogeneous reactions between chlorine reservoir species (e.g. HCl and $ClONO_2$) produce active, ozone-destroying chlorine radicals. Furthermore, sulfate aerosols are the basis for polar stratospheric cloud formation, and thus influence ozone chemistry during the polar night and in spring (Carslaw et al., 1997). The resultant decreases in ozone then also affect climate at Earth's surface **(Son et al., 2010)**.

Major volcanic eruptions such as the eruption of Mt. Pinatubo in the Philippines in June 1991 inject large amounts of sulfur dioxide (SO_2) into the stratosphere, where SO_2 is oxidised to form sulfuric acid (H_2SO_4). Because of the extremely low vapour pressure of H_2SO_4-H_2O solutions at lower stratospheric temperatures, gaseous H_2SO_4 quickly condenses forming sulfate aerosol particles. The Mt. Pinatubo eruption is frequently studied owing to good observational coverage at that point in time. Two to four months after the eruption, the lower tropical stratosphere warmed by up to 3.5 K (Labitzke and McCormick, 1992), and global-mean surface temperatures decreased by approximately 0.4 K (Robock and Mao, 1995). Column ozone decreased by 5–10% over the globe, with large losses observed at northern midlatitudes and in the tropics (Randel et al., 1995). Small increases in ozone were initially observed at southern midlatitudes**, which is thought to be** due to the aerosol-induced increase in tropical upwelling and subsequent enhanced transport of ozone by Southern Hemisphere extratropical downwelling (Aquila et al., 2013).

Because aerosols play such an important role in Earth's climate, as observed from past volcanic eruptions **e.g.** (Robock, 2000; Guillet et al., 2017; Solomon et al., 2011), it is vitally important that their effects on the atmosphere can be accurately simulated. Satellite-based measurements of stratospheric aerosol properties have been available since 1979, and from these global, spatially resolved values for aerosol surface area density (SAD), mass and mean radius can be derived, albeit only with large uncertainties because the aerosol size distribution is under-determined by the extinction or backscatter information.

These quantities are needed to drive global circulation and chemistry-climate models (GCMs and CCMs), which are used for simulating aerosol effects on climate. However, model simulations of the Mt. Pinatubo eruption are diverse. For example, **GCMs participating in phase 5 of the Coupled Model Intercomparison Project (CMIP5) simulated tropical (30° N–30° S) temperature anomalies at 50 hPa ranging between 2–10 K (Driscoll et al., 2012). Similarly, CCMs** ~~the~~ CCMs participating in CCMVal-2, the predecessor activity to phase 1 of the Chemistry-Climate Model Initiative (CCMI-1), simulated global-mean temperature anomalies between -1 K and +9 K at 50 hPa in the post-Pinatubo eruption period, and global-mean ozone anomalies between -2% and -22% (Mancini et al., 2010). While this is partly due to how the models handle aerosol radiative and chemical processes, the process of compiling the best historic stratospheric aerosol data set with which to drive the models is also incomplete. Kremser et al. (2016) discuss the challenges inherent in constructing a long-term stratospheric aerosol climatology, a process which is further complicated by the fact that following a major volcanic eruption, the lower stratosphere is too optically thick for occultation instruments onboard satellites to make accurate measurements, so that a gap-filling procedure is required for the opaque regions.

Here we evaluate stratospheric aerosol data sets produced for two major modelling activities, CCMI-1 and ~~phase 6 of the Coupled Model Intercomparison Project (~~CMIP6~~)~~. For the ongoing CCMI-1 activity, CCMs are evaluated to obtain projections of the stratospheric ozone layer, tropospheric composition, air quality, global climate change and the interactions between them (Morgenstern et al., 2017). For CMIP6, participating GCMs and CCMs provide projections of how the Earth system responds to forcing, and how climate may change in future (Eyring et al., 2016). Here we analyse CCM simulations forced with SAGE-4λ and SAGE-3λ, the stratospheric aerosol data sets that were developed for CCMI-1 and CMIP6, respectively. We investigate the impact of the Mt. Pinatubo eruption on ~~climate and~~ stratospheric chemistry **and temperatures** as simulated with the two stratospheric aerosol data sets. The results indicate that stratospheric temperatures and ozone changes induced by the Mt. Pinatubo eruption in simulations based on SAGE-3λ for CMIP6 are in better agreement with observations than the simulations based on SAGE-4λ for CCMI-1, which in turn is better than previous aerosol data sets based on SAGE retrieval versions 5.9 or earlier (Arfeuille et al., 2013).

2 Stratospheric aerosol data sets

To simulate the effects of stratospheric aerosol on chemistry and climate, GCMs and CCMs need temporally and spatially resolved values of aerosol radiative properties as a function of wavelength spanning the electromagnetic spectrum from the ultraviolet to the infrared, and information about the aerosol size distribution such as SAD and mean radii. **This was done previously by e.g. (Bauman, 2003a, b) and (Bingen, 2004a, a).** The stratospheric aerosol data sets developed for CCMI-1 and CMIP6 are summarized in Table 1, and described in more detail below.

2.1 SAGE-4λ: CCMI stratospheric aerosol data set

The CCMI stratospheric aerosol data set (Luo, 2013) was prepared for models participating in CCMI-1 (Morgenstern et al., 2017). This data set covers the period 1960–2010, and is based on SAGE (Stratospheric Aerosol and Gas Experiment) II ex-

tinction data. It constructs single mode lognormal aerosol size distributions by means of the SAGE-4λ algorithm (Section 2.3), which uses all four wavelengths (385, 452, 525 and 1024 nm) of SAGE II data when available. In times before and after SAGE II (October 1984–August 2005) other satellite measurements are used. Since satellite measurements became available only in 1979, for volcanically quiescent periods prior to 1979, the monthly mean background aerosol measured by SAGE II during the volcanic quiescent period 1996–2005 is used. Volcanic contributions are calculated using the AER-2D model for spatial and temporal evolution (Arfeuille et al., 2014). Stratospheric aerosol optical depths are calibrated using photometer data when available. From 1979 onwards, the data set is based on satellite measurements from the SAM, SAGE I, and SAGE II instruments, followed by CALIPSO after 2005, which was when SAGE II measurements ended. Ground-based Lidar measurements supplement SAGE II data following the Mt. Pinatubo eruption, when much of the lower stratosphere was too opaque for SAGE II to measure (Arfeuille et al., 2013). The SAGE-4λ data set and description can be found at ftp://iacftp.ethz.ch/pub_read/luo/ccmi/.

2.2 SAGE-3λ: CMIP6 stratospheric aerosol data set

The CMIP6 stratospheric aerosol data set was prepared for models participating in CMIP6 (Eyring et al., 2016), including the ongoing Model Intercomparison Project on the climatic response to Volcanic forcing (VolMIP) (Zanchettin et al., 2016). In the CMIP6 stratospheric aerosol data set, which spans from 1850–2015, SAD and radiative properties are derived via the SAGE-3λ algorithm similar to SAGE-4λ, but omitting the less reliable channel at 385 nm (see below). Similar to the CCMI data set, for volcanically quiescent periods prior to 1979, the monthly mean background aerosol measured by SAGE II during the volcanic quiescent period 1996–2005 is used, and volcanic contributions are calculated using the AER-2D model for spatial and temporal evolution (Arfeuille et al., 2014), calibrated by photometer data when available. From 1979 onwards, the data set is based on satellite measurements from the SAM, SAGE I, SAGE II, CALIPSO and OSIRIS instruments. CLAES (Cryogenic Limb Array Etalon Spectrometer) measurements are used for data-filling following the Mt. Pinatubo eruption. Furthermore, one additional correction is applied in SAGE-3λ that is missing in SAGE-4λ: in the extra-tropical lowermost stratosphere tiny particles ($r < 10$ nm), which hardly scatter or absorb sunlight and are practically invisible to satellites, but contribute significantly to SAD, are corrected based on optical particle counter (OPC) data (Deshler et al., 2003). This correction is applied below 20 km **at all latitudes and seasons** to SAD, volume density, mean radius and H_2SO_4 mass. No correction is made for the radiative properties, as the tiny particles hardly influence the radiative balance. (We note that we apply the original OPC data and do not use the new derivations of size distributions by Kovilakam and Deshler (2015), as they slightly overestimate SAD during volcanic periods). The SAGE-3λ data set and description can be found at ftp://iacftp.ethz.ch/pub_read/luo/CMIP6/.

2.3 SAGE-3~~,~~4λ and SAGE-4λ algorithms

The SAGE-4λ and SAGE-3λ algorithms were used in the CCMI and CMIP6 data sets, respectively. In both cases, a lognormal size distribution of stratospheric aerosol is assumed. For a single mode lognormal distribution, three parameters (number density n, mode radius r and width σ) are required. Both the SAGE-3λ and SAGE-4λ algorithms consist of two steps bffor calculating n, r and σ:

1) Obtain n, r and σ by fitting the SAGE II extinction coefficients at four wavelengths (385, 452, 525 and 1024 nm) for the CCMI data set and three wavelengths for the CMIP6 data set. The data uncertainty at 385 nm is much higher than for the other three wavelengths, for two reasons. Firstly, the molecular extinction at shorter wavelengths is higher than at longer wavelengths. Therefore the removal of the signal of air molecules is much more difficult. Secondly, the extinction at 385 nm is also affected by gas phase absorption. Therefore, in the more recent CMIP6 data set, the extinction coefficients at 385 nm are excluded.

2) ~~Using the SAGE II data, a correction for effective radius (r_{eff}) and σ with an extinction coefficient at wavelength 1020 nm (k_{1020}) is obtained. During the SAGE II time period, the remaining two parameters were calculated using the r_{eff}–k_{1020} correlation for the CCMI data set and σ–k_{1020} correlation for the CMIP6 data set. For other time periods, extinction coefficients at only one wavelength were available (from satellite instruments or photometers). Both correlations, again obtained from the SAGE II time period, were used to calculate the remaining unknown parameter, the number density.~~ **In step 1, n, r and σ were obtained using the extinction coefficients at three wavelengths for the CMIP6 data set, and four wavelengths for the CCMI data set, which are partially correlated. However, a small measurement error on the input values may cause large inaccuracies in the output parameters (n, r and σ). Therefore a σ–k_{1020} correlation was used in the CMIP6 data set to minimize the effects introduced by the measurement errors, even during the SAGE II period, where extinction coefficients at three wavelengths were available. This correlation is obtained from the output of step 1. In CCMI, the r_{eff}–k_{1020} correlation was used to obtain r. The remaining two parameters (n and σ) were obtained by fitting to the measured extinction coefficients. The fitting quality remains almost as good as step 1.**

For other time periods (outside the SAGE II period), extinction coefficients at only one wavelength were available (from satellite instruments or photometers). Both correlations (σ–k_{1020} and r_{eff}–k_{1020}), again obtained from the SAGE II time period, were used to calculate the remaining unknown parameter, the number density. At pre-photometer times, volcanic aerosol inputs were simulated using the AER stratospheric aerosol model (Arfeuille et al., 2014).

The radiative properties (extinction coefficients, single scattering albedos and asymmetry factors) for model wavelength bands were then calculated using Mie theory (Bohren and Huffman, 2007). For SOCOLv3 this procedure was executed for 6 wavelength bands in the shortwave range (solar radiation) and 16 in the longwave range (terrestrial radiation).

3 Chemistry-Climate Model and simulations

Simulations were performed with version 3 of the Solar Climate Ozone Links (SOCOLv3) CCM, which participated in CCMI-1 (Morgenstern et al., 2017). The base version of the CCM is described in detail and validated against observations by Stenke et al. (2013). Since then, SOCOLv3's tropospheric chemistry scheme was upgraded (Revell et al., 2015) and the model formulation was updated for participation in CCMI-1, which led to improvements in SOCOLv3's simulation of key stratospheric variables such as temperature and water vapour concentration (Revell et al., 2016). For this study, SOCOLv3 was run with 39 vertical levels between the Earth's surface and 80 km ($\sim$0.01 hPa) and T42 horizontal resolution, which corresponds to latitude/longitude grid spacing of $2.8^\circ \times 2.8^\circ$.

Aerosol radiative effects are calculated within SOCOLv3 by using pre-calculated extinction coefficients, asymmetry factors and single scattering albedos for each spectral band to derive radiative heating rates**, scattering and atmospheric transmission**. Radiative transfer calculations are performed by the shortwave radiation scheme of Fouquart and Bonnel (1980), using three spectral bands in the UV-visible range and three bands in the near-IR (NIR) range (Cagnazzo et al., 2007). For the long-wave part of the spectrum the RRTM (Rapid Radiative Transfer Model) by Mlawer et al. (1997) including 16 bands is used. In the stratosphere, aerosol effects on heterogeneous chemistry are taken into account by using SAD and mean aerosol radius provided within the CCMI and CMIP6 stratospheric aerosol data sets. In the troposphere an aerosol data set is prescribed (Anet et al., 2013) which affects radiation but not heterogeneous chemistry. SAD is set to zero in the troposphere, and aerosol radiative properties merge from the stratospheric to the tropospheric data sets through two transition layers at the WMO-defined tropopause. In the lower transition layer two-thirds of the prescribed tropospheric aerosol is used in combination with one-third of the prescribed stratospheric aerosol. In the upper transition layer these proportions are reversed, so that one-third of the prescribed tropospheric aerosol is used together with two-thirds stratospheric aerosol.

To better understand the chemical versus dynamical effects on stratospheric ozone following the eruption of Mt. Pinatubo, the ozone destruction rates of the gas-phase catalytic NO_x, reactive hydrogen (HO_x=H+OH+HO_2) and reactive chlorine (Cl_x=Cl+ClO+2$\times$$Cl_2O_2$+$ClONO_2$) cycles were tracked as a function of latitude, longitude, pressure and time as described in detail by Revell et al. (2012); see their Supporting Information for a list of the chemical cycles tracked.

Two ensembles of SOCOLv3 simulations were performed, a "CCMI" ensemble and a "CMIP6" ensemble. Each ensemble consists of five SOCOLv3 simulations, where for each simulation the initial CO_2 concentration was perturbed slightly to explore the model's internal variability. Both ensembles used boundary conditions recommended for the CCMI-1 reference simulation REF-C1, except that the simulations performed for the "CMIP6" ensemble used the stratospheric aerosol data set that was prepared for CMIP6. The REF-C1 simulation is a free-running simulation (i.e., meteorology evolves without nudging to reanalyses) of the recent past, as described in detail by Morgenstern et al. (2017). Greenhouse gas concentrations follow observations until 2005, then follow Representative Concentration Pathway (RCP) 8.5 (Masui et al., 2011). Historical ozone precursor emissions are used until 2000 (Lamarque et al., 2010), and then follow RCP 6.0 (Meehl et al., 2013). Sea surface temperatures and sea ice concentrations are prescribed following observations until 2003 (Rayner et al., 2003), and then follow RCP 6.0. Halogen-containing ozone-depleting substances follow the A1 scenario from WMO (2011) which includes observations until 2009. **Although the REF-C1 simulation is free-running, in SOCOLv3 the quasi-biennial oscillation (QBO) is forced by nudging the zonal tropical stratospheric winds (20° N–20° S, 3–90 hPa) to a time series of observed wind profiles (Giorgetta, 1996; Stenke et al., 2013).**

Three of the "CCMI" simulations ran for the full REF-C1 period from 1960–2010 and have been uploaded to the CCMI archive (ETH-PMOD, 2015) (excluding the model spin-up period from 1950–1959). The other seven simulations ran from 1986–2005 to focus on the Mt. Pinatubo eruption period, and have been uploaded to a separate online repository (Kuchar and Revell, 2017). Here we focus on the common period, i.e. 1986–2005 for each simulation, and examine anomalies following the Mt. Pinatubo eruption. Anomalies are calculated by removing the annual cycle averaged over 1986–2005. This approach

does not completely isolate the volcanic signal, but allows a consistent comparison between data obtained from SOCOLv3, observations and reanalyses.

4 Results and Discussion

4.1 Difference in aerosol mass in the CCMI and CMIP6 aerosol data sets

We first of all compare the SAGE-4λ and SAGE-3λ stratospheric aerosol data sets used for CCMI and CMIP6, respectively. The relative difference in H_2SO_4 aerosol mass is shown in Fig. 1. Differences in aerosol mass loading are due to the different gap-filling procedures used following the Mt. Pinatubo eruption. Lidar data were used for gap-filling in the SAGE-4λ data set, while CLAES data were predominantly used for the SAGE-3λ data set (Lidar measurements were occasionally used but only in the tropics). Stark differences exist between aerosol loading in the two data sets in June 1991 (Fig. 1b), because in the SAGE-3λ data set, missing data between 20° N–20° S were gap-filled by replicating May 1991 data, thus effectively moving the timing of the Pinatubo eruption to July 1991 (Thomason et al., 2017).

Differences in aerosol loading lead to changes in stratospheric heating due to absorption of longwave radiation by aerosols. In the CMIP6 data set there is approximately twice as much aerosol loading in the tropical middle stratosphere (around 30–50 hPa) than in the CCMI data set (Fig. 1e–h). However in the tropical lower stratosphere, just above the tropical tropopause, there is ~~approximately five times less~~ **only half as much** aerosol in the CMIP6 data set ~~than in~~ **compared to** the CCMI data set. ~~Changes in heating where the stratosphere is coldest, i.e. the lower stratosphere, have a larger impact on heating than higher in the stratosphere where it is warmer.~~

4.2 Ensemble simulations using the CCMI aerosol data set

Changes in stratospheric temperature, dynamics and chemistry following the Mt. Pinatubo eruption have been documented extensively (Pitari and Rizi, 1993; Kinnison et al., 1994; Randel et al., 1995; Rosenfield et al., 1997; Rozanov et al., 2002; Aquila et al., 2013; Pitari et al., 2014). Here we examine how the Mt. Pinatubo eruption is simulated with SOCOLv3 using the SAGE-4λ stratospheric aerosol data set for CCMI, and then compare the post-eruption changes in temperature, chemistry and dynamics with the simulations using the SAGE-3λ stratospheric aerosol data set for CMIP6.

Ensemble-, zonal-mean anomalies in temperature, ozone concentrations and the rate of the vertical residual circulation for the CCMI ensemble are shown in Figure 2. Averaged over the six months following the Mt. Pinatubo eruption, volcanic aerosol causes heating in the lower stratosphere of approximately up to 4 K via absorption of NIR solar radiation and outgoing longwave radiation (Fig. 2a). Heating in the tropical stratosphere **is thought to** drive~~s~~ an increase in the rate of tropical upwelling (Rosenfield et al., 1997), indicated by an increase in the residual vertical velocity w* (Fig. 2b), which is a useful proxy for the strength of the Brewer-Dobson circulation. As well as increased tropical upwelling, downwelling in the Southern Hemisphere is enhanced during the six months following the eruption, which is consistent with the findings of Aquila et al. (2013) and

Dhomse et al. (2015). Stronger tropical upwelling leads to the ozone maximum shifting upwards, causing localized reductions in tropical ozone concentrations of 0.4 ppmv ($\sim$10%) centered at 30 hPa (Fig. 2c).

Stratospheric ozone is not only influenced by changes in the rate of tropical upwelling but also by stratospheric composition changes following the eruption. Heterogeneous chemical reactions on the surface of aerosol particles convert active NO_x to reservoir species, and reservoir chlorine to active Cl_x (i.e. HCl + $ClONO_2$ $\rightarrow$ Cl_2 + HNO_3, followed by photolysis of Cl_2 to produce Cl radicals). With increased conversion of NO_x to reservoir species, the gas-phase ozone destroying NO_x cycles slow, less ClO is converted to $ClONO_2$, and thus the Cl_x cycles become faster. This can be seen in Fig. 2d, which shows anomalies in the tropical zonal-mean rates of the gas-phase NO_x, HO_x and Cl_x ozone destruction cycles. Between 10–50 hPa, NO_x-induced ozone destruction slows by up to 40% in the 6 months following the eruption, indicating increased NO_x deactivation. This results in a faster rate of HO_x- and Cl_x-induced ozone loss, as shown previously by e.g. Rodriguez et al. (1991) and Tie and Brasseur (1995). HO_x chemistry is also faster because the tropical cold-point tropopause warms following the eruption and the flux of water vapour into the stratosphere increases (Löffler et al., 2016). At 30 hPa the net chemical effect is reduced ozone destruction due to NO_x deactivation, as shown by the black trace in Fig. 2d. However the overall effect on tropical ozone at 30 hPa is driven by the dynamical effect, i.e. a localized reduction due to uplift of ozone caused by increased tropical upwelling. The chlorine activation effect can be seen just above 100 hPa in Fig. 2d, where increased abundances of Cl_x lead to the rate of the Cl_x-induced ozone loss cycles accelerating by up to 150%. Although this is a large relative increase, the absolute increase is small as the gas-phase chlorine cycles are generally slow in the lowermost stratosphere (not shown).

4.3 Comparison of simulations using the CCMI and CMIP6 aerosol data sets

Having shown in general terms how SOCOLv3 simulates the Mt. Pinatubo eruption, we now examine the specific differences induced by the CCMI and CMIP6 stratospheric aerosol data sets. Ensemble mean differences between temperature, w*, ozone and the rate of ozone destruction chemistry in the CCMI and CMIP6 simulations are shown in Fig. 3. **(Absolute ensemble-, zonal-mean anomalies in temperature, w* and ozone for the CMIP6 simulations are shown in the supplement).** While the stratosphere warms by up to 4 K in the CCMI ensemble (Fig. 2a), the tropical warming is only $\sim$2 K in the CMIP6 ensemble (Fig. 3a), due to less aerosol mass loading in the tropical lower stratosphere (Fig. 1). Concurrently, the tropical vertical residual circulation strengthens less in the CMIP6 ensemble compared with the CCMI ensemble (Fig. 3b), which leads to less dynamical uplift of ozone-rich air, and a smaller local ozone reduction in the middle stratosphere is simulated (Fig. 3c and 4b).

We also examine the difference in the NO_x and Cl_x chemical ozone destruction rates following the eruption between the CCMI and CMIP6 ensembles (Fig. 3d). It is expected that differences in aerosol mass and SAD between the CMIP6 and CCMI stratospheric aerosol data sets lead to differences in the rate of heterogeneous chemical reactions. This can be seen clearly in the rate of the Cl_x cycles in the tropical lower stratosphere. Because there is less aerosol mass in the tropical lower stratosphere in the CMIP6 data set compared with the CCMI data set, there is less chlorine activation, and therefore Cl_x-induced ozone destruction is significantly slower. In the middle stratosphere more NO_x deactivation, and therefore less NO_x-induced ozone destruction, occurs in the CCMI ensemble compared with the CMIP6 ensemble.

Finally, tropical temperature and ozone anomalies as simulated with SOCOLv3 are compared with reanalyses and observations (Fig. 4). We focus on the 30 hPa level as the preceding figures indicate that this is the pressure level around which significant differences between ozone and temperature in the two ensembles are centered. **Furthermore, latitude/pressure cross-sections for temperature reanalyses data sets and ozone observations are shown in the supplement, and these confirm that the anomalies peak at 30 hPa.** Compared to MERRA and ERA-Interim reanalysis data, simulations using the CCMI aerosol data set overestimate the temperature response to the Mt. Pinatubo eruption by ∼3 K, which was also shown by Arfeuille et al. (2013) and Kuchar et al. (2017). The CMIP6 ensemble simulates tropical warming of ∼2 K following the eruption, which is in good agreement with ERA-Interim (Dee et al., 2011) and MERRA (Rienecker et al., 2011) reanalyses (Fig. 4a), and also with CCM simulations using a new database of volcanic SO_2 emissions and plume altitudes (Mills et al., 2016).

The CMIP6 ensemble simulations of ozone in the post-eruption period show a better agreement with observations than the simulations based on the CCMI data set (Fig. 4b). Merged satellite observations from the Stratospheric Water and Ozone Satellite Homogenized (SWOOSH) data set (Davis et al., 2016) show ozone decreasing by ∼0.4 ppmv six months after the eruption. The CCMI ensemble overestimates ozone loss in this period by up to 0.2 ppmv, while the CMIP6 ensemble agrees more closely with observations, and overestimates ozone loss only by ∼0.1 ppmv.

5 Conclusions

We have used two stratospheric aerosol data sets developed for the model intercomparison activities CCMI-1 and CMIP6 to drive SOCOLv3 CCM simulations of the Mt. Pinatubo eruption. Following the eruption, aerosol mass injected into the lower stratosphere absorbs infrared radiation and heats the stratosphere. This in turn **may** ~~leads to~~ strengthen~~ed~~ tropical upwelling and lift~~s~~ the ozone maximum in the tropics, causing a localized reduction in ozone around 30 hPa. In the simulations using the SAGE-4λ stratospheric aerosol data set developed for CCMI, **tropical** stratospheric **warming following the Mt. Pinatubo eruption** is overestimated by approximately 3 K compared to reanalyses, and local reductions in ozone are overestimated by approximately 0.2 ppmv. Because of different gap-filling procedures used for the lower stratosphere following the Mt. Pinatubo eruption, the SAGE-3λ data set developed for CMIP6 contains less aerosol mass in the lower stratosphere compared with the CCMI data set. Therefore in the model simulations using CMIP6 stratospheric aerosol, the stratosphere warms less than it does in the simulations with CCMI stratospheric aerosol. Using CMIP6 stratospheric aerosol, SOCOLv3 simulates a warming of approximately 2 K following the Mt. Pinatubo eruption that is in good agreement with reanalyses. While ozone loss is overestimated compared to observations, it is in closer agreement with observations than the results from the simulations using CCMI stratospheric aerosol.

The CCM simulations presented here indicate that using the SAGE-3λ stratospheric aerosol data set developed for CMIP6 in SOCOLv3 leads to an improved simulation of **tropical** stratospheric temperature and ozone changes following the Mt. Pinatubo eruption compared with the simulations using the SAGE-4λ stratospheric aerosol data set developed for CCMI.

However, various CCMs and GCMs calculate the radiative and chemical effects of aerosols on the stratosphere in different ways, and the two stratospheric aerosol data sets should therefore be used within other models to validate our conclusions.

Data availability. SOCOL v.3 CCMI-1 REF-C1 data are held at the British Atmospheric Data Centre, see http://catalogue.ceda.ac.uk/uuid/1005d2c25d14483aa66a5f4a7f50fcf0. All other simulations can be found at ~~https://data.mendeley.com/datasets/khrhbw6wn5/draft?a=35729334-ca37-4434-bd26-60dadfb9c22b~~ **https://data.mendeley.com/datasets/khrhbw6wn5/1**.

Author contributions. BL and TP were involved in developing the SAGE-4λ and SAGE-3λ data sets. AS, ER and TS were involved in developing the SOCOLv3 CCM. AS devised the experiments. LER performed the model simulations and analysed the data. LER led the writing of this manuscript, assisted by SK and all other co-authors.

Competing interests. The authors declare no competing interests.

Acknowledgements. LER thanks Larry Thomason for helpful discussions around this paper. ER and TS acknowledge support from the Swiss National Science Foundation under grant 200021_169241 (VEC).

References

Anet, J. G., Rozanov, E. V., Muthers, S., Peter, T., Brönnimann, S., Arfeuille, F., Beer, J., Shapiro, A. I., Raible, C. C., Steinhilber, F., and Schmutz, W. K.: Impact of a potential 21st century "grand solar minimum" on surface temperatures and stratospheric ozone, Geophys. Res. Lett., 40, 4420-4425, doi:10.1002/grl.50806, 2013.

Aquila, V., Oman, L.D., Stolarski, R., Douglass, A.R., and Newman, P.A.: The response of ozone and nitrogen dioxide to the eruption of Mt. Pinatubo at southern and northern midlatitudes, J. Atmos. Sci., 70, 894-900, doi:10.1175/jas-d-12-0143.1, 2013.

Arfeuille, F., Luo, B. P., Heckendorn, P., Weisenstein, D., Sheng, J. X., Rozanov, E., Schraner, M., Brönnimann, S., Thomason, L. W., and Peter, T.: Modeling the stratospheric warming following the Mt. Pinatubo eruption: Uncertainties in aerosol extinctions, Atmos. Chem. Phys., 13, 11,221-11,234, doi:10.5194/acp-13-11221-2013, 2013.

Arfeuille, F., Weisenstein, D., Mack, H., Rozanov, E., Peter, T., and Brönnimann, S.: Volcanic forcing for climate modeling: a new microphysics-based data set covering years 1600–present, Clim. Past, 10, 359-375, doi:10.5194/cp-10-359-2014, 2014.

Bauman, J.J., Russell, P.B., Geller, M.A. and Hamill, P.: A stratospheric aerosol climatology from SAGE II and CLAES measurements: 1. Methodology, J. Geophys. Res., 108, 4382, doi:10.1029/2002JD002992, 2003.

Bauman, J.J., Russell, P.B., Geller, M.A. and Hamill, P.: A stratospheric aerosol climatology from SAGE II and CLAES measurements: 2. Results and comparisons, 1984–1999, J. Geophys. Res., 108, 4383, doi:10.1029/2002JD002993, 2003.

Bingen, C., Fussen, D. and Vanhellemont, F.: A global climatology of stratospheric aerosol size distribution parameters derived from SAGE II data over the period 1984–2000: 1. Methodology and climatological observations, J. Geophys. Res., 109, D06201, doi:10.1029/2003JD003518, 2004.

Bingen, C., Fussen, D. and Vanhellemont, F.: A global climatology of stratospheric aerosol size distribution parameters derived from SAGE II data over the period 1984–2000: 2. Reference data, J. Geophys. Res., 109, D06202, doi:10.1029/2003JD003511, 2004.

Bohren, C.F., and Huffman, D.R.: Absorption and Scattering of Light by Small Particles, Wiley-VCH, Berlin, doi:10.1002/9783527618156, 2007.

Boucher, O., Randall, D., Artaxo, P., Bretherton, C., Feingold, G., Forster, P., Kerminen, V.-M., Kondo, Y., Liao, H., Lohmann, U., Rasch, P., Satheesh, S. K., Sherwood, S., Stevens, B., and Zhang, X.Y.: Clouds and Aerosols. In: Climate Change 2013: The Physical Science Basis. Contribution of Working Group I to the Fifth Assessment Report of the Intergovernmental Panel on Climate Change [Stocker, T.F., Qin, D., Plattner, G.-K., Tignor, M., Allen, S.K., Boschung, J., Nauels, A., Xia, Y., Bex, V., and Midgley, P.M. (eds.)]. Cambridge University Press, Cambridge, United Kingdom and New York, NY, USA, 2013.

Cagnazzo, C., Manzini, E., Giorgetta, M.A., de F. Forster, P.M., and Morcrette, J.-J.: Impact of an improved radiation scheme in the MAECHAM5 General Circulation Model, Atmos. Chem. Phys., 7, 2503-2515, doi:10.5194/acp-7-2503-2007, 2007.

Carslaw, K.S., Peter, T., and Clegg, S.L.: Modeling the composition of liquid stratospheric aerosols, Rev. Geophys., 35, 125-154, doi:10.1029/97RG00078, 1997.

Davis, S.M., Rosenlof, K.H., Hassler, B., Hurst, D.F., Read, W.G., Vömel, H., Selkirk, H., Fujiwara, M., and Damadeo, R.: The Stratospheric Water and Ozone Satellite Homogenized (SWOOSH) database: a long-term database for climate studies, Earth Syst. Sci. Data, 8, 461-490, doi:10.5194/essd-8-461-2016, 2016.

Dee, D.P., Uppala, S.M., Simmons, A.J., Berrisford, P., Poli, P., Kobayashi, S., Andrae, U., Balmaseda, M.A., Balsamo, G., Bauer, P., Bechtold, P., Beljaars, A.C.M., van de Berg, L., Bidlot, J., Bormann, N., Delsol, C., Dragani, R., Fuentes, M., Geer, A.J., Haimberger, L., Healy, S.B., Hersbach, H., Hólm, E.V., Isaksen, L., Kallberg, P., Köhler, M., Matricardi, M., McNally, A.P., Monge-Sanz, B.M., Morcrette,

J.-J., Park, B.-K., Peubey, C., de Rosnay, P., Tavolato, C., Thépaut, J.-N., and Vitart, F.: The ERA-Interim reanalysis: configuration and performance of the data assimilation system, Q.J.R. Meteorol. Soc., 137, 553-597, doi:10.1002/qj.828, 2011.

Deshler, T., Hervig, M.E., Hofmann, D.J., Rosen, J.M. and Liley, J.B.: Thirty years of in situ stratospheric aerosol size distribution measurements from Laramie, Wyoming (41° N), using balloon-borne instruments, J. Geophys. Res.-Atmos., 108, D5, doi:10.1029/2002JD002541, 2003.

Dhomse, S.S., Chipperfield, M.P., Feng, W., Hossaini, R., Mann, G.W., and Santee, M.L.: Revisiting the hemispheric asymmetry in midlatitude ozone changes following the Mount Pinatubo eruption: A 3-D model study, Geophys. Res. Lett., 42, 3038-3047, doi:10.1002/2015GL063052, 2015.

Driscoll, S., Bozzo, A., Gray, L.J., Robock, A. and Stenchikov, G.: Coupled Model Intercomparison Project 5 (CMIP5) simulations of climate following volcanic eruptions, J. Geophys. Res., 117, D17105, doi:10.1029/2012JD017607, 2012.

ETH-PMOD: Swiss Federal Institute of Technology Zurich and the Physical-Meteorology Observatory Davos, Data, Part of the Chemistry-Climate Model Initiative (CCMI-1) Project Database, NCAS British Atmospheric Data Centre, available at: http://catalogue.ceda.ac.uk/uuid/1005d2c25d14483aa66a5f4a7f50fcf0 (last access: 20 April 2017), 2015.

Eyring, V., Bony, S., Meehl, G.A., Senior, C.A., Stevens, B., Stouffer, R.J., and Taylor, K.E.: Overview of the Coupled Model Intercomparison Project Phase 6 (CMIP6) experimental design and organization, Geosci. Model Dev., 9, 1937-1958, doi:10.5194/gmd-9-1937-2016, 2016.

Fouquart, Y., and Bonnel, B.: Computations of solar heating of the Earth's atmosphere - A new parameterization, Beitr. Phys. Atmos., 53, 35-62, 1980.

Giorgetta, M. A.: Der Einfluss der quasi-zweijährigen Oszillation: Modellrechnungen mit ECHAM4, Max-Planck-Institut für Meteorologie, Hamburg, Examensarbeit Nr. 40, MPI-Report 218, 1996.

Guillet, S., Corona, C., Stoffel, M., Khodri, M., Lavigne, F., Ortega, P., Eckert, N., Sielenou, P. D., Daux, V., Churakova (Sidorova), O. V., Davi, N., Edouard, J.-L., Zhang, Y., Luckman, B. H., Myglan, V. S., Guiot, J., Beniston, M., Masson-Delmotte, V., and Oppenheimer, C.: Climate response to the Samalas volcanic eruption in 1257 revealed by proxy records, Nat. Geosci., 10, 123-138, doi:10.1038/ngeo2875, 2017.

Kinnison, D.E., Grant, K.E., Connell, P.S., Rotman, D.A., and Wuebbles, D.J.: The chemical and radiative effects of the Mount Pinatubo eruption, J. Geophys. Res.: Atmos., 99, 25705-25731, doi:10.1029/94JD02318, 1994.

Kovilakam, M., and Deshler, T.: On the accuracy of stratospheric aerosol extinction derived from in situ size distribution measurements and surface area density derived from remote SAGE II and HALOE extinction measurements, J. Geophys. Res.: Atmos., 120, 8426-8447, doi:10.1002/2015JD023303, 2015.

Kremser, S., Thomason, L.W., von Hobe, M., Hermann, M., Deshler, T., Timmreck, C., Toohey, M., Stenke, A., Schwarz, J.P., Weigel, R., Fueglistaler, S., Prata, F.J., Vernier, J.-P., Schlager, H., Barnes, J.E., Antuña-Marrero, J.-C., Fairlie, D., Palm, M., Mahieu, E., Notholt, J., Rex, M., Bingen, C., Vanhellemont, F., Bourassa, A., Plane, J.M.C., Klocke, D., Carn, S.A., Clarisse, L., Trickl, T., Neely, R., James, A.D., Rieger, L., Wilson, J.C., and Meland, B.: Stratospheric aerosol–Observations, processes, and impact on climate, Rev. Geophys., 54, 278-335, doi:10.1002/2015RG000511, 2016.

Kuchar, A., Ball, W., Rozanov, E., Stenke, A., Revell, L., Miksovsky, J., Pisoft, P., and Peter, T.: On the aliasing of the solar cycle in the lower-stratospheric tropical temperature, J. Geophys. Res.-Atmos., under review, 2017.

Kuchar, A., and Revell, L.: SOCOLv3 model data for "On the aliasing of the solar cycle in the lower-stratospheric tropical temperature" and "Chemistry-climate model simulations of the Mt. Pinatubo eruption using CCMI and CMIP6 stratospheric aerosol data sets", http://dx.doi.org/10.17632/khrhbw6wn5.1, doi:10.17632/khrhbw6wn5.1, 2017.

Labitzke, K., and McCormick, M.P.: Stratospheric temperature increases due to Pinatubo aerosols, Geophys. Res. Lett., 19, 207-210, doi:10.1029/91GL02940, 1992.

Lamarque, J.-F., Bond, T. C., Eyring, V., Granier, C., Heil, A., Klimont, Z., Lee, D., Liousse, C., Mieville, A., Owen, B., Schultz, M. G., Shindell, D., Smith, S. J., Stehfest, E., Van Aardenne, J., Cooper, O. R., Kainuma, M., Mahowald, N., McConnell, J. R., Naik, V., Riahi, K., and van Vuuren, D. P.: Historical (1850–2000) gridded anthropogenic and biomass burning emissions of reactive gases and aerosols: methodology and application, Atmos. Chem. Phys., 10, 7017-7039, doi:10.5194/acp-10-7017-2010, 2010.

Löffler, M., Brinkob, S., and Jöckel, P.: Impact of major volcanic eruptions on stratospheric water vapour, Atmos. Chem. Phys., 16, 6547-6562, doi:10.5194/acp-16-6547-2016, 2016.

Luo, B.: Stratospheric aerosol data for use in CCMI models, available at: ftp://iacftp.ethz.ch/pub_read/luo/ccmi/ (last access: 20 April 2017), 2013.

Mancini, E., Matthes, K., Blume, C., Bodeker, G., Cagnazzo, C., Calvo, N., Charlton-Perrez, A., Douglass, A., Fogli, P. G., Gray, L., Kim, J., Kodera, K., Kunze, M., Pena-Ortiz, C., Randel, B., Reichler, T., Stenchikov, G., Timmreck, C., Toohey, M., and Yoden, S.: Natural Variability of Stratospheric Ozone. In: SPARC Report on the Evaluation of Chemistry-Climate Models, edited by: Eyring, V., Shepherd, T. G. and Waugh, D. W., SPARC Report No. 5, WCRP-132, WMO/TD-No. 1526, available at: http://www.sparc-climate.org/publications/sparc-reports/sparc-report-no5/ (last access: 6 April 2017), 2010.

Masui, T., Matsumoto, K. Hijioka, Y., Kinoshita, T., Nozawa, T., Ishiwatari, S., Kato, E., Shukla, P. R., Yamagata, Y., and Kainuma, M.: An emission pathway for stabilization at 6 Wm^{-2} radiative forcing, Climatic Change, 109, 59-76, doi:10.1007/s10584-011-0150-5, 2011.

Meehl, G. A., Washington, W. M., Arblaster, J. M., Hu, A., Teng, H., Kay, J. E., Gettelman, A., Lawrence, D. M., Sanderson, B. M., and Strand, W. G.: Climate change projections in CESM1(CAM5) compared to CCSM4, J. Climate, 26, 6287-6308, doi:10.1175/JCLI-D-12-00572.1, 2013.

Mills, M.J., Schmidt, A., Easter, R., Solomon, S., Kinnison, D.E., Ghan, S. J., Neely, R.R., Marsh, D.R., Conley, A., Bardeen, C.G., and Gettelman, A.: Global volcanic aerosol properties derived from emissions, 1990–2014, using CESM1(WACCM), J. Geophys. Res.:Atmos., 121, 2232-2348, doi:10.1002/2015JD02490, 2016.

Mlawer, E.J., Taubman, S.J., Brown, P.D., Iacono, M.J., and Clough, S.A.: Radiative transfer for inhomogeneous atmospheres: RRTM, a validated correlated-k model for the longwave, J. Geophys. Res.: Atmos., 102, 16663-16682, doi:10.1029/97JD00237, 1997.

Morgenstern, O., Hegglin, M.I., Rozanov, E., O'Connor, F.M., Abraham, N.L., Akiyoshi, H., Archibald, A.T., Bekki, S., Butchart, N., Chipperfield, M.P., Deushi, M., Dhomse, S.S., Garcia, R.R., Hardiman, S.C., Horowitz, L.W., Jöckel, P., Josse, B., Kinnison, D., Lin, M., Mancini, E., Manyin, M.E., Marchand, M., Marécal, V., Michou, M., Oman, L.D., Pitari, G., Plummer, D.A., Revell, L.E., Saint-Martin, D., Schofield, R., Stenke, A., Stone, K., Sudo, K., Tanaka, T.Y., Tilmes, S., Yamashita, Y., Yoshida, K., and Zeng, G.: Review of the global models used within phase 1 of the Chemistry-Climate Model Initiative (CCMI), Geosci. Model Dev., 10, 639-671, doi:10.5194/gmd-10-639-2017, 2017.

Muthers, S., Arfeuille, F., Raible, C.C., and Rozanov, E.: The impacts of volcanic aerosol on stratospheric ozone and the Northern Hemisphere polar vortex: separating radiative-dynamical changes from direct effects due to enhanced aerosol heterogeneous chemistry, Atmos. Chem. Phys., 15, 11461-11476, doi:10.5194/acp-15-11461-2015, 2015.

Pitari, G., Aquila, V., Kravitz, B., Robock, A., Watanabe, S., Cionni, I., Luca, N.D., Genova, G.D., Mancini, E., and Tilmes, S.: Stratospheric ozone response to sulfate geoengineering: Results from the Geoengineering Model Intercomparison Project (GeoMIP), J. Geophys. Res.: Atmos., 119, 2629-2653, doi:10.1002/2013JD020566, 2014.

Pitari, G., and Rizi, V.: An estimate of the chemical and radiative perturbation of stratospheric ozone following the eruption of Mt. Pinatubo, J. Atmos. Sci., 50, 3260-3276, doi:10.1175/1520-0469(1993)050<3260:aeotca>2.0.co;2, 1993.

Randel, W.J., Wu, F., Russell, J.M., Waters, J.W., and Froidevaux, L.: Ozone and temperature changes in the stratosphere following the eruption of Mount Pinatubo, J. Geophys. Res.: Atmos., 100, 16753-16764, doi:10.1029/95JD01001, 1995.

Rayner, N. A., Parker, D. E., Horton, E. B., Folland, C. K., Alexander, L. V., Rowell, D. P., Kent, E. C., and Kaplan, A.: Global analyses of sea surface temperature, sea ice, and night marine air temperature since the late nineteenth century, J. Geophys. Res., 108, 4407, doi:10.1029/2002JD002670, 2003.

Revell, L.E., Bodeker, G.E., Smale, D., Lehmann, R., Huck, P.E., Williamson, B.E., Rozanov, E., and Struthers, H.: The effectiveness of N_2O in depleting stratospheric ozone, Geophys. Res. Lett., 39, doi:10.1029/2012GL052143, 2012.

Revell, L.E., Tummon, F., Stenke, A., Sukhodolov, T., Coulon, A., Rozanov, E., Garny, H., Grewe, V., and Peter, T.: Drivers of the tropospheric ozone budget throughout the 21^{st} century under the medium-high climate scenario RCP 6.0, Atmos. Chem. Phys., 15, 5887-5902 doi:10.5194/acp-15-5887-2015, 2015.

Revell, L.E., Stenke, A., Rozanov, E., Ball, W., Lossow, S., and Peter, T.: The role of methane in projections of 21^{st} century stratospheric water vapour, Atmos. Chem. Phys., 16, 13067-13080 doi:10.5194/acp-16-13067-2016, 2016.

Rienecker, M.M., Suarez, M.J., Gelaro, R., Todling, R., Bacmeister, J., Liu, E., Bosilovich, M.G., Schubert, S.D., Takacs, L., Kim, G.-K., Bloom, S., Chen, J., Collins, D., Conaty, A., da Silva, A., Gu, W., Joiner, J., Koster, R.D., Lucchesi, R., Molod, A., Owens, T., Pawson, S., Pegion, P., Redder, C.R., Reichle, R., Robertson, F.R., Ruddick, A.G., Sienkiewicz, M., and Woollen, J.: MERRA: NASA's Modern-Era Retrospective Analysis for Research and Applications, J. Climate, 24, 3624-3648, doi:10.1175/jcli-d-11-00015.1, 2011.

Robock, A., and Mao, J.: The volcanic signal in surface temperature observations, J. Climate, 8, 1086-1103, doi:10.1175/1520-0442(1995)008<1086:tvsist>2.0.co;2, 1995.

Robock, A.: Volcanic eruptions and climate, Rev. Geophys., 38(2), 191–219, doi:10.1029/1998RG000054, 2000.

Rodriguez, J.M., Ko, M.K.W., and Sze, N.D.: Role of heterogeneous conversion of N_2O_5 on sulphate aerosols in global ozone losses, Nature, 352, 134-137, doi:10.1038/352134a0, 1991.

Rosenfield, J.E., Considine, D.B., Meade, P.E., Bacmeister, J.T., Jackman, C.H., and Schoeberl, M.R.: Stratospheric effects of Mount Pinatubo aerosol studied with a coupled two-dimensional model, J. Geophys. Res.: Atmos., 102, 3649-3670, doi:10.1029/96JD03820, 1997.

Rozanov, E., Schlesinger, M.E., Andronova, N.G., Yang, F., Malyshev, S.L., Zubov, V.A., Egorova, T.A., and Li, B.: Climate/chemistry effects of the Pinatubo volcanic eruption simulated by the UIUC stratosphere/troposphere GCM with interactive photochemistry, J. Geophys. Res., 107(D21), 4594, doi:10.1029/2001JD000974, 2002.

Solomon, S., Daniel, J.S., Neely, R.R., Vernier, J.-P., Dutton, E.G., and Thomason, L.W.: The persistently variable "background" stratospheric aerosol layer and global climate change, Science, 333, 866-870, doi:10.1126/science.1206027, 2011.

Son, S.-W., Gerber, E.P., Perlwitz, J., Polvani, L.M., Gillett, N.P., Seo, K.-H., Eyring, V., Shepherd, T.G., Waugh, D., Akiyoshi, H., Austin, J., Baumgaertner, A., Bekki, S., Braesicke, P., Brühl, C., Butchart, N., Chipperfield, M.P., Cugnet, D., Dameris, M., Dhomse, S., Frith, S., Garny, H., Garcia, R., Hardiman, S.C., Jöckel, P., Lamarque, J. F., Mancini, E., Marchand, M., Michou, M., Nakamura, T., Morgenstern, O., Pitari, G., Plummer, D.A., Pyle, J., Rozanov, E., Scinocca, J.F., Shibata, K., Smale, D., Teyssédre, H., Tian, W., and Yamashita, Y.: Impact of stratospheric ozone on Southern Hemisphere circulation change: A multimodel assessment, J. Geophys. Res., 115, D00M07, doi:10.1029/2010JD014271, 2010.

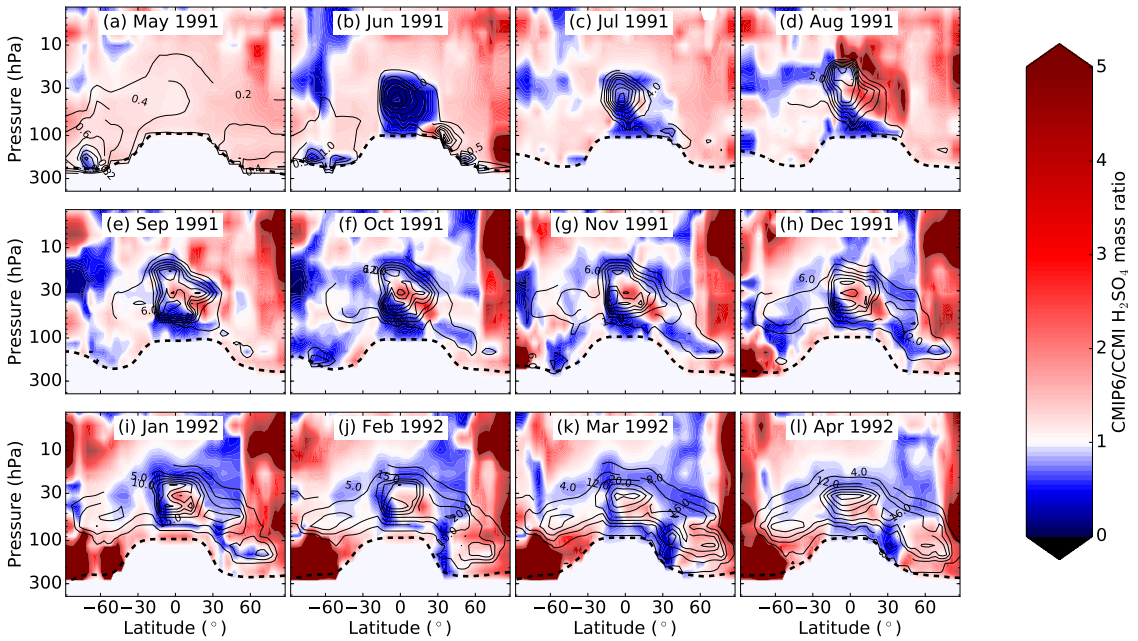

Figure 1. ~~Ratio of~~ **Percent difference in** H_2SO_4 aerosol mass in the CCMI and CMIP6 stratospheric aerosol data sets for 12 months around the Mt. Pinatubo eruption in June 1991, CMIP6~~/~~**minus**CCMI. Black contours show the CCMI H_2SO_4 mass in 10^9 molecules cm^{-3}. The dashed black line shows the location of the WMO-defined tropopause. Note that aerosol data are supplied down to 5 km altitude in the CCMI and CMIP6 data sets, which are based on cloud-cleared SAGE II measurements, but these values are recommended for use only above the model tropopause.

Stenke, A., Schraner, M., Rozanov, E., Egorova, T., Luo, B., and Peter, T.: The SOCOL version 3.0 chemistry-climate model: description, evaluation, and implications from an advanced transport algorithm, Geosci. Model Dev., 6, 1407-1427, doi:10.5194/gmd-6-1407-2013, 2013.

Thomason, L. W., Ernest, N., Millán, L., Rieger, L., Bourassa, A., Vernier, J.-P., Manney, G., Luo, B., Arfeuille, F., and Peter, T.: A global, space-based stratospheric aerosol climatology: 1979 to 2016, Earth Syst. Sci. Data Discuss., https://doi.org/10.5194/essd-2017-91, in review, 2017.

Tie, X., and Brasseur, G.: The response of stratospheric ozone to volcanic eruptions: Sensitivity to atmospheric chlorine loading, Geophys. Res. Lett., 22, 3035-3038, doi:10.1029/95GL03057, 1995.

World Meteorological Organization: Scientific Assessment of Ozone Depletion: 2010, WMO Global Ozone Research and Monitoring Project - Report No. 52, Geneva, Switzerland, 2011.

Zanchettin, D., Khodri, M., Timmreck, C., Toohey, M., Schmidt, A., Gerber, E.P., Hegerl, G., Robock, A., Pausata, F.S.R., Ball, W.T., Bauer, S.E., Bekki, S., Dhomse, S.S., LeGrande, A.N., Mann, G.W., Marshall, L., Mills, M., Marchand, M., Niemeier, U., Poulain, V., Rozanov, E., Rubino, A., Stenke, A., Tsigaridis, K., and Tummon, F.: The Model Intercomparison Project on the climatic response to Volcanic forcing (VolMIP): experimental design and forcing input data for CMIP6, Geosci. Model Dev., 9, 2701-2719, doi:10.5194/gmd-9-2701-2016, 2016.

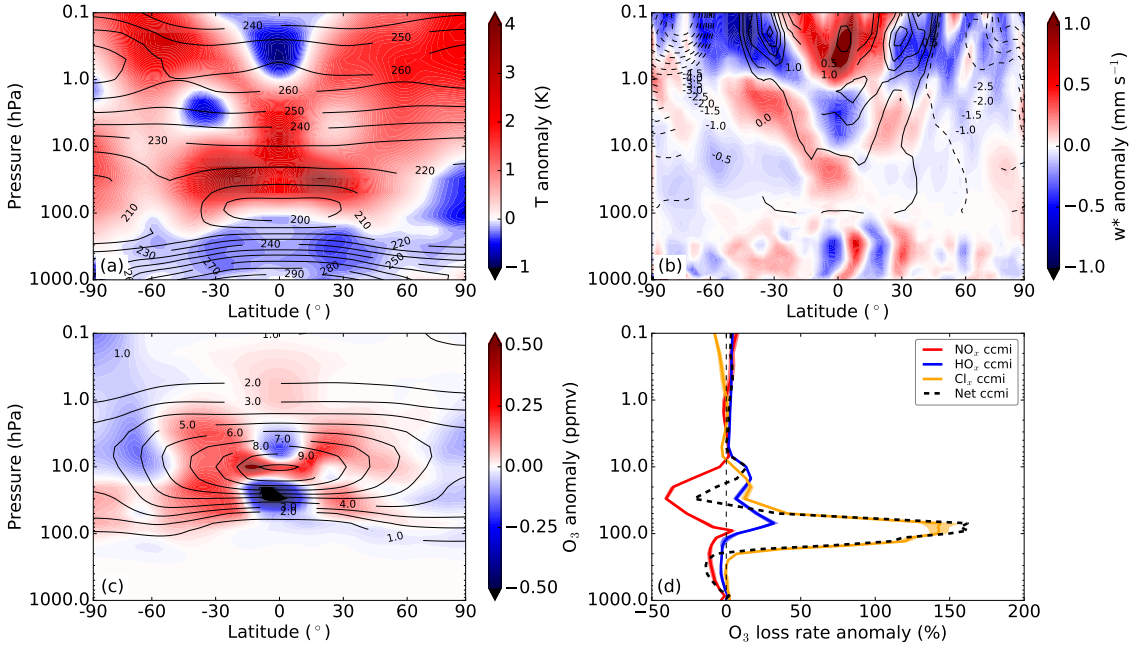

Figure 2. Ensemble-mean, zonal-mean anomalies averaged over the 6 months following the Mt. Pinatubo eruption for the simulations using CCMI aerosol. (a) Temperature anomalies in the CCMI ensemble (red/blue shading). Black contours indicate the annual climatological mean (1986-2005) temperatures for the CCMI ensemble. (b) As for (a), but showing anomalies in the rate of the vertical residual circulation (w*). For clarity, the annual climatological mean rate of the vertical residual circulation (black contours) is only shown above 100 hPa. Dashed contours indicate negative values. (c) As for (a), but showing ozone anomalies. (d) Anomalies in tropical (15°N –15° S) ozone destruction rates by the NO_x, HO_x and Cl_x ozone destruction cycles. Negative anomalies indicate slower ozone destruction. Shading indicates the ensemble standard deviation. The dashed black line shows the sum of the NO_x, HO_x and Cl_x anomalies, i.e. the net anomaly in the ozone destruction rate following the eruption.

Table 1. Stratospheric aerosol data sets used for CCMI-1 and CMIP6.

	SAGE-4λ data set for CCMs in CCMI-1	**SAGE-3λ data set for GCMs and CCMs in CMIP6**
Period	1960-2010	1850-2015
Data used	SAM, SAGE I, SAGE II, CALIPSO; sun-photometer data; AER stratospheric aerosol model.	SAM, SAGE I, SAGE II, SAM, CALIPSO, OSIRIS; sun-photometer data; AER stratospheric aerosol model; mass, volume density, SAD, r_{eff} corrected for very small particles below 20 km by OPC measurements.
Data gap filling following the Mt. Pinatubo eruption	Lidar measurements	Predominantly CLAES observations

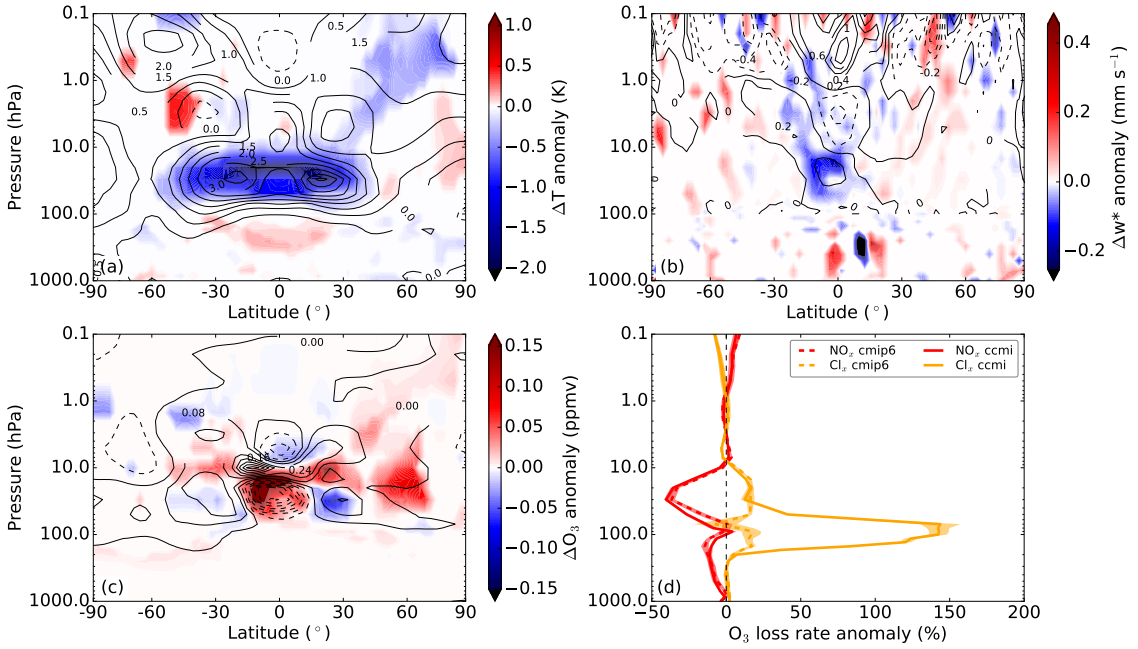

Figure 3. Differences in ensemble-mean, zonal-mean anomalies averaged over the 6 months following the Mt. Pinatubo eruption between the ensembles using CMIP6 and CCMI aerosol (CMIP6 minus CCMI). For the contour plots (a-c), regions that are not statistically significant at the 95% level of confidence (as calculated with Student's t test, $p<0.05$) are set to zero. (a) Difference in temperature anomalies (red/blue shading). For reference, the black contours represent the CCMI anomalies over the same period, i.e., the red/blue shading from Fig. 2a. (b) As for (a), but showing anomalies in the vertical residual circulation. (c) As for (a), but showing ozone anomalies. (d) As for Fig. 2d, but showing anomalies in the tropical ozone destruction rates for only the NO_x and Cl_x ozone destruction cycles in the CMIP6 and CCMI ensembles.

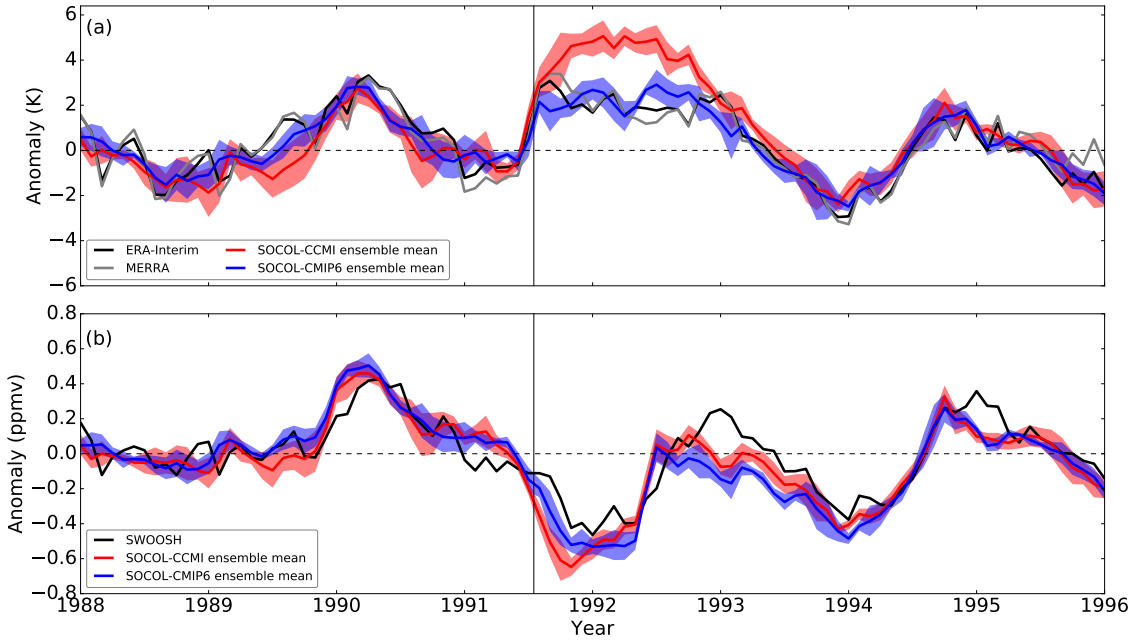

Figure 4. Time series of (a) temperature and (b) ozone anomalies at 30 hPa, 15° N–15° S. The red and blue lines denote the ensemble mean of the SOCOLv3 CCMI and CMIP6 ensembles, respectively. The shaded areas denote the ensemble mean plus or minus one standard deviation of simulated anomalies, and the vertical lines show the timing of the Mt. Pinatubo eruption on 15 June 1991.

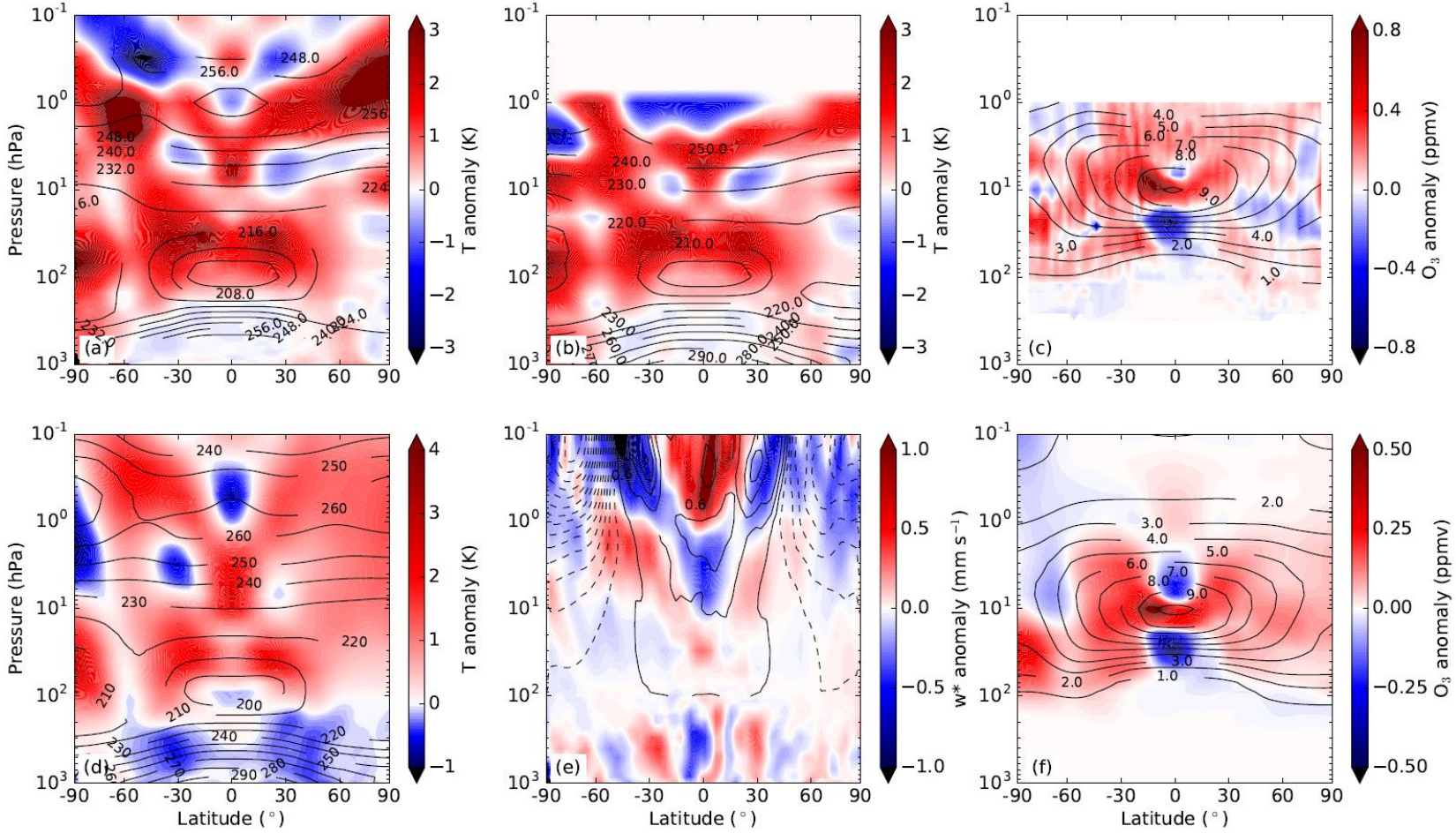

Top row: Zonal-mean anomalies in the 6 months following the Mt. Pinatubo eruption for (a) MERRA temperature reanalyses; (b) ERA-Interim temperature reanalyses; (c) SWOOSH ozone observations. Black contour lines show the annual climatological mean (1986-2005). **Bottom row:** As for Figure 2(a-c), but for the simulations using CMIP6 stratospheric aerosol. i.e., ensemble-mean, zonal-mean anomalies averaged over the 6 months following the Mt. Pinatubo eruption. (d) Temperature anomalies in the CMIP6 ensemble (red/blue shading). Black contours indicate the annual climatological mean (1986-2005) temperatures for the CMIP6 ensemble. (e) As for (d), but showing anomalies in the rate of the vertical residual circulation (w*). For clarity, the annual climatological mean rate of the vertical residual circulation (black contours) is only shown above 100 hPa. Dashed contours indicate negative values. (f) As for (d), but showing ozone anomalies.